EPJ Web of Conferences **75**, 04009 (2014)
DOI: 10.1051/epjconf/20147504009
© Owned by the authors, published by EDP Sciences, 2014

Ordered phase formation in Sm-Ni thin film deposited on Cr(100) single-crystal underlayer

Yusuke Hotta[1,a], Makoto Yamada[1], Takato Yanagawa[1], Mitsuru Ohtake[1], Fumiyoshi Kirino[2], Nobuyuki Inaba[3], and Masaaki Futamoto[1]

[1]Faculty of Science and Engineering, Chuo University, 1-13-27 Kasuga, Bunkyo-ku, Tokyo 112-8551, Japan
[2]Graduate School of Fine Arts, Tokyo University of the Arts, 12-8 Ueno-koen, Taito-ku, Tokyo 110-8714, Japan
[3]Faculty of Engineering, Yamagata University, 4-3-16 Jyonan, Yonezawa 992-8510, Japan

Abstract. $Sm_{17}Ni_{83}$ (at. %) alloy thin films are prepared on Cr(100) underlayers hetero-epitaxially grown on MgO(100) single-crystal substrates by employing an ultra-high vacuum molecular beam epitaxy system. The effect of substrate temperature on the ordered phase formation is investigated. The films deposited below 300 °C consist of amorphous phase, whereas formation of $SmNi_5$ ordered phase is recognized for the films deposited above 400 °C. The $SmNi_5$ films with ordered phase consist of two types of $(11\bar{2}0)$ variant whose *c*-axes are lying in the film plane and rotated around the film normal by 90° each other. With increasing the temperature from 400 to 500 °C, the long-range order degree increases from 0.65 to 0.80. The ordered film formed at 500 °C shows an in-plane magnetic anisotropy reflecting the magnetocrystalline anisotropy of $SmNi_5$ crystal.

1 Introduction

Magnetic thin films with the uniaxial magnetocrystalline anisotropy energy (K_u) greater than 10^7 erg/cm^3 and with the easy magnetization axis parallel to the substrate surface have been investigated for nanocomposite magnets. In order to control the easy magnetization direction, well-defined epitaxial films are useful, since the crystallographic orientation of film can be controlled by that of single-crystal substrate. $SmCo_5$ alloy with RT_5 ordered structure shows K_u of 1.1×10^8 erg/cm^3 along the *c*-axis [1]. $SmCo_5$ epitaxial films with the *c*-axis lying in in-plane have been prepared on MgO(100) [2–5] and MgO(110) [3–6] substrates by employing W [4], Cr [2, 3], and Fe [5, 6] underlayers. In our previous studies [7, 8], $SmCo_5$ epitaxial films with the *c*-axes parallel and perpendicular to the substrate surface were respectively prepared on Cr and Cu underlayers by employing a molecular beam epitaxy (MBE) system equipped with a reflection high-energy electron diffraction (RHEED) facility. *In-situ* RHEED revealed the crystallographic property during film formation, which varied depending not only the substrate temperature but also on the film thickness.

The Sm and Co sites in $SmCo_5$ structure can be replaced with other rare earth metal (R) and transition metal (T) elements, respectively. The structural and magnetic properties are considered to vary depending on the combination of T and R elements. Epitaxial RCo_5 (R = Pr, Nd, etc.) ordered epitaxial films have been prepared [9, 10], whereas there are few reports on the formation of SmT_5 (T = Fe, Ni) ordered films [11–13].

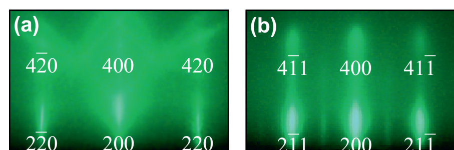

Fig. 1. RHEED patterns observed for (a) an MgO(100) substrate and (b) an Cr underlayer deposited on the substrate at 500 °C.

Ni (1455 °C) has a lower melting point than Co (1495 °C) and Fe (1538 °C). Atomic diffusion activity of metal element is sometimes related with the melting point which reflects the atomic binding force. Ni atoms are thus considered to diffuse more easily and to have a lower activation energy in forming the SmT_5 compound. In the present study, $Sm_{17}Ni_{83}$ (at. %) films are deposited on Cr(100) single-crystal underlayers. The effects of substrate temperature and film thickness on the ordered phase formation are investigated.

2 Experimental procedure

Thin films were prepared on polished MgO(100) substrates by using an MBE system. The base pressures were lower than 7×10^{-9} Pa. Before film formation, substrates were heated at 500 °C for 1 h to obtain clean surfaces. Figure 1(a) shows the RHEED pattern observed for a substrate after heating. The RHEED pattern exhibits a *Kikuchi* pattern, indicating that the surface is clean and smooth. Pure Ni (99.99%) was evaporated by electron beam heating, whereas pure Sm (99.9%) and Cr (99.9%) were evaporated by using Knudsen cells. The film layer

[a] Corresponding author: hotta@futamoto.elect.chuo-u.ac.jp

This is an Open Access article distributed under the terms of the Creative Commons Attribution License 2.0, which permits unrestricted use, distribution, and reproduction in any medium, provided the original work is properly cited.

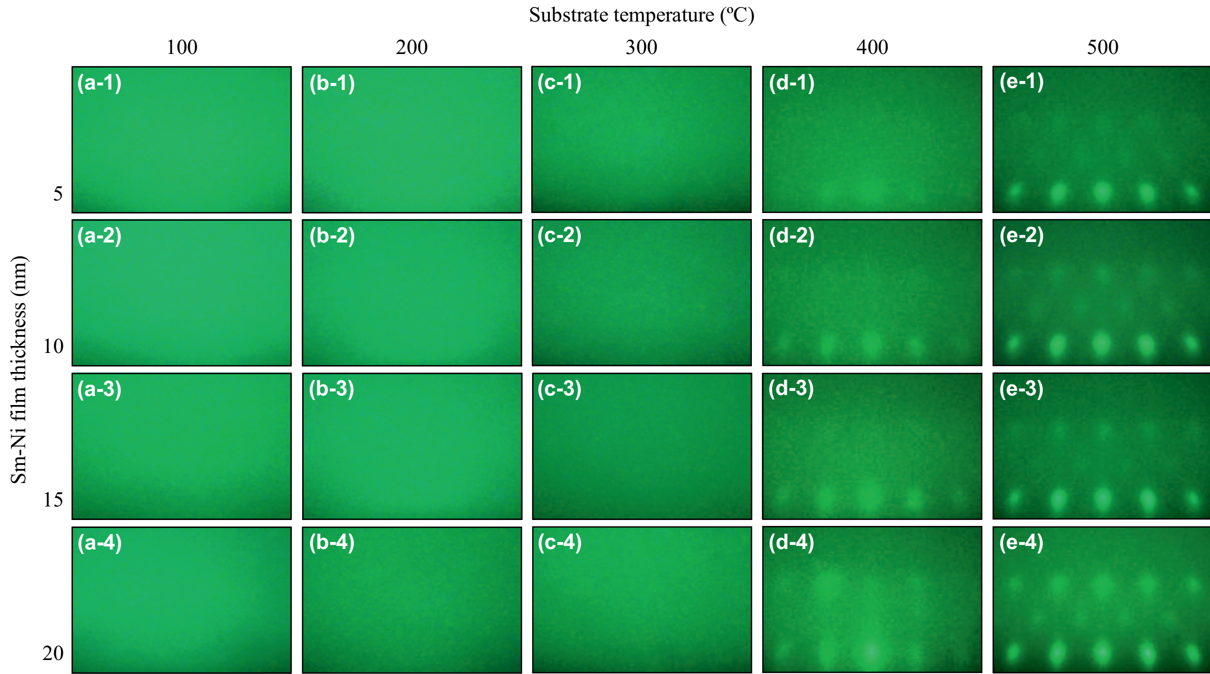

Fig. 2. RHEED patterns observed during Sm-Ni deposition on Cr(100) underlayers at (a) 100, (b) 200, (c) 300, (d) 400, and (e) 500 °C. The film thicknesses are (a-1)–(e-1) 5, (a-2)–(e-2) 10, (a-3)–(e-3) 15, and (a-4)–(e-4) 20 nm. The incident electron beam is parallel to Cr[011].

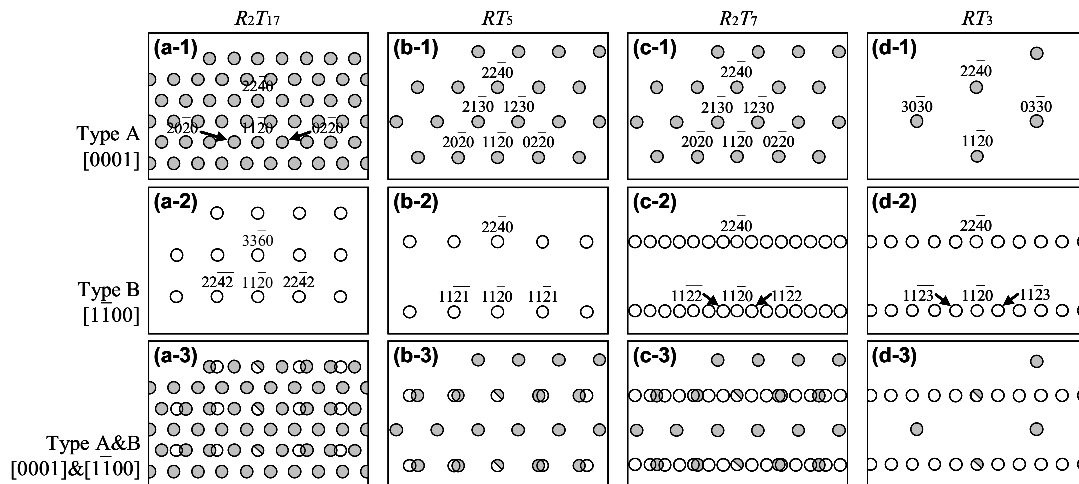

Fig. 3. Schematic diagrams of RHEED patterns simulated for Sm-Ni(11$\bar{2}$0) surfaces with (a) R_2T_{17}-, (b) RT_5-, (c) R_2T_7- and (d) RT_3-type structures by using the lattice constants of bulk Sm_2Ni_{17} (a = 0.8380 nm, c = 0.8106 nm [14]), $SmNi_5$ (a = 0.4926 nm, c = 0.3980 nm [15]), Sm_2Ni_7 (a = 0.4969 nm, $c/6$ = 0.4058 nm [16]), and $SmNi_3$ (a = 0.5005 nm, $c/6$ = 0.41 nm [16]) crystals. The incident electron beam is parallel to (a-1)–(d-1) [0001] or (a-2)–(d-2) [1$\bar{1}$00]. Schematic diagrams of (a-3)–(d-3) are drawn by overlapping (a-1)–(d-1) and (a-2)–(d-2), respectively.

structure is $Sm_{17}Ni_{83}$(20 nm)/Cr(20 nm)/MgO. A Cr underlayer of 20 nm thickness was deposited on the substrate at 500 °C. Figure 1(b) shows the RHEED pattern observed for a Cr underlayer deposited on MgO substrate. A clear diffraction pattern corresponding to bcc(100) texture is recognized. The epitaxial orientation relationship of Cr(100)[011] ∥ MgO(100)[001] is determined. An Cr(100) single-crystal underlayer is formed. A 20-nm-thick Sm-Ni film with the Sm composition of 17 at. % which is almost the $SmNi_5$ stoichiometry was deposited on the Cr(100) underlayer at a substrate temperature in a range between 100 and 500 °C. The Sm-Ni film compositions were confirmed by energy dispersive X-ray spectroscopy and the errors were less than 1 at. % from the $SmNi_5$ stoichiometry.

The surface structure during film deposition was observed by RHEED. The resulting film structure was investigated by $2\theta/\omega$-scan out-of-plane and $2\theta\chi/\varphi$-scan in-plane X-ray diffrections (XRDs) with Cu-Kα radiation (λ = 0.15418 nm). The magnetization curves were measured by using a vibrating sample magnetometer.

3 Results and discussion

Figures 2(a)–(c) show the RHEED patterns observed during Sm-Ni deposition on Cr(100) underlayers at temperatures ranging between 100 and 300 °C. Diffuse diffraction patterns are recognized. The result shows that amorphous Sm-Ni films are formed. Figure 2(d) shows the RHEED patterns observed for an Sm-Ni film deposited at 400 °C. The RHEED patterns correspond to a diffraction pattern from RT_5(11$\bar{2}$0) surface [figure 3(b)] and do not correspond to formations of (11$\bar{2}$0) crystals with hexagonal

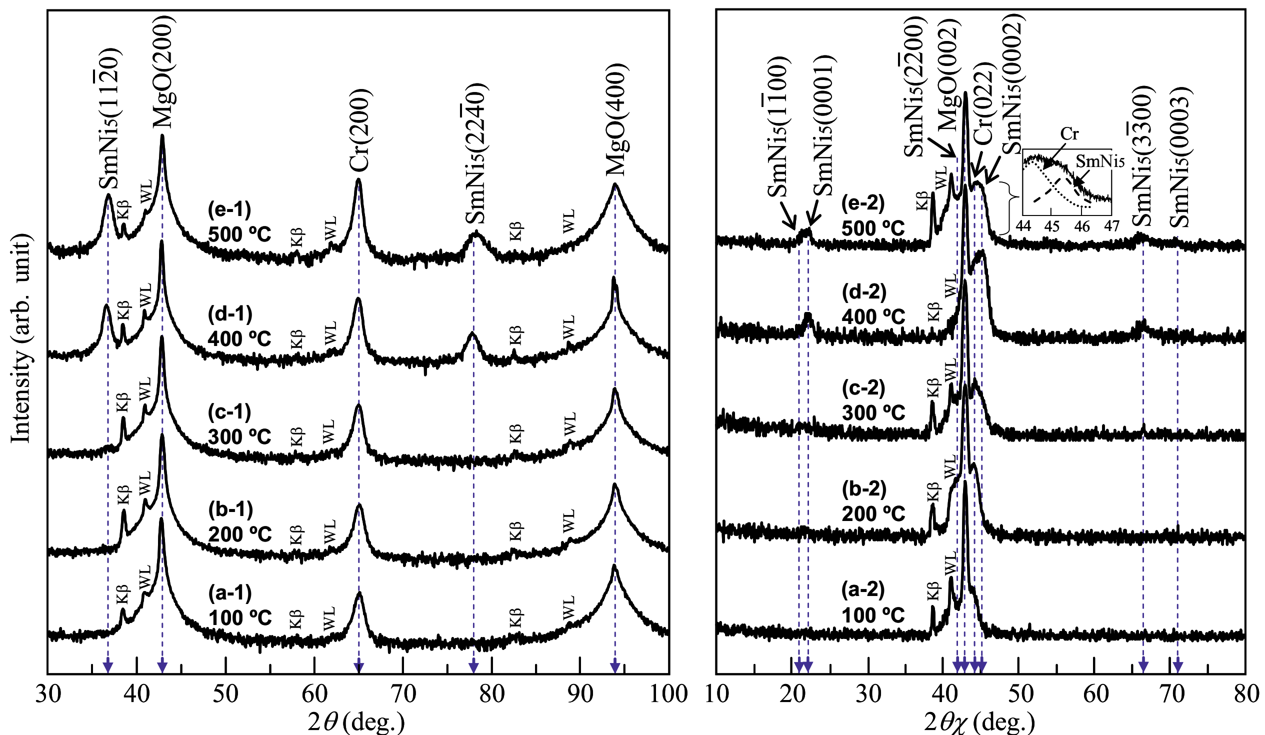

Fig. 4. (a-1)–(e-1) Out-of-plane and (a-2)–(e-2) in-plane XRD patterns of Sm-Ni films deposited on Cr(100) underlayers at (a) 100, (b) 200, (c) 300, (d) 400, and (e) 500 °C. The scattering vector is parallel to (a-1)–(e-1) MgO[100] or (a-2)–(e-2) MgO[001]. The intensity shown in a logarithmic scale. The small reflections noted as Kβ and WL are due to Cu-Kβ and W-Lα radiations included in the X-ray source, respectively.

R_2T_{17}-, R_2T_7-, and RT_3-type structures [figures 3(a, c, d)]. An Sm-Ni epitaxial film consisting of only RT_5 ordered phase is obtained at 400 °C. The ordered phase formation is enhanced with increasing the substrate temperature. The RHEED pattern is analyzed to be an overlap of two reflections, as shown by the filled and open circles in figure 3(b). The epitaxial orientation relationship is determined as

$$SmNi_5(11\bar{2}0)[0001] \parallel Cr(100)[011] \text{ (type A)},$$

$$SmNi_5(11\bar{2}0)[1\bar{1}00] \parallel Cr(100)[011] \text{ (type B)}.$$

The film consists of two types of $(11\bar{2}0)$ variant whose *c*-axes are lying in the film plane and rotated around the film normal by 90° each other. In this configuration, the lattice mismatch differs depending on the in-plane direction. The mismatches at the $SmNi_5$/Cr interface along $SmNi_5[0001]$ and $SmNi_5[1\bar{1}00]$ are respectively calculated to be –2.4% and +5.0%, where the lattice constants of bulk $SmNi_5$ (a = 0.4926 nm, c = 0.3980 nm [15]) and Cr (a = 0.2884 nm [17]) crystals are used. Although there exists such a large misfit of –5.0% along $SmNi_5[1\bar{1}00]$, epitaxial growth of $SmNi_5$ crystal on Cr(100) underlayer is taking place. With increasing the Sm-Ni film thickness from 5 to 20 nm, the sharpness of RHEED pattern gradually increases. The result suggests that the film is strained around the $SmNi_5$/Cr interface due to the lattice mismatch and the strain decreases with increasing the thickness. Figure 2(e) shows the RHEED patterns observed for an Sm-Ni film deposited at 500 °C. A clear diffraction pattern corresponding to $RT_5(11\bar{2}0)$ texture is recognized through the course of deposition. The diffraction spots are sharper when compared with those observed for the film deposited at 400 °C. The film strain is decreased by employing a higher substrate temperature.

Figures 4(a-1)–(e-1) show the out-of-plane XRD patterns. No reflections from Sm-Ni crystals are observed for the films deposited below 300 °C [figures 4(a-1)–(c-1)] due to that the films consist of amorphous phase. $SmNi_5(11\bar{2}0)$ and $SmNi_5(22\bar{4}0)$ fundamental reflections are recognized for the films deposited above 400 °C [figures 4(d-1, e-1)]. The values of full width at half maximum of ω-scan rocking curves of films deposited at 400 and 500 °C measured by fixing the diffraction angle of 2θ at the peak angle of $SmNi_5(11\bar{2}0)$ reflection are 2.84° and 2.67°, respectively. With increasing the substrate temperature from 400 to 500 °C, the film strain decreases.

Figures 4(a-2)–(e-2) show the in-plane patterns measured by making the scattering vector parallel to MgO[001]. For the films deposited above 400 °C, $SmNi_5(0001)$ and $SmNi_5(0003)$ superlattice reflections are observed in addition to $SmNi_5(0002)$, $SmNi_5(1\bar{1}00)$, $SmNi_5(2\bar{2}00)$, and $SmNi_5(3\bar{3}00)$ fundamental reflections. The in-plane XRD confirms the formation of $SmNi_5$ ordered phase and the epitaxial orientation relationship which are determined by RHEED. The in-plane lattice spacings of ($d_{SmNi5(0001)}$, $d_{SmNi5(1\bar{1}00)}$) of films deposited at 400 and 500 °C are (0.4017, 0.4247) and (0.4033, 0.4187), respectively. The $d_{SmNi5(0001)}$ and the $d_{SmNi5(1\bar{1}00)}$ values of these films are respectively larger and smaller than those of bulk $SmNi_5$ crystal ($d_{SmNi5(0001)}$ = 0.3980 nm, $d_{SmNi5(1\bar{1}00)}$ = 0.4266 nm [15]). This is due to an influence of lattice mismatches at the $SmNi_5$/Cr interface along $SmNi_5[0001]$ (–2.4%) and $SmNi_5[1\bar{1}00]$ (+5.0%). The lattice constants of (a_1, a_2, a_3, c) = ($[(d_{SmNi5(1\bar{1}00)})^2+(d_{SmNi5(11\bar{2}0)})^2]^{1/2}$, $[(d_{SmNi5(0001)})^2+(d_{SmNi5(1\bar{1}00)})^2]^{1/2}$, $2d_{SmNi5(11\bar{2}0)}$, $d_{SmNi5(0001)}$) of films deposited at 400 and 500 °C are calculated to be (0.4906 nm, 0.5846 nm, 0.4911 nm, 0.4017 nm) and (0.4848 nm, 0.5813 nm, 0.4887 nm, 0.4033 nm), respectively.

Long-range order degree (S) of $SmNi_5$ phase is

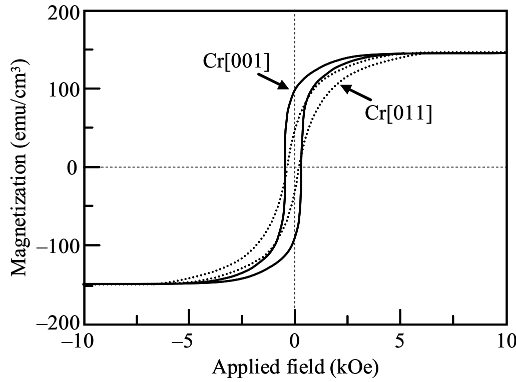

Fig. 5. Magnetization curves measured for an $SmNi_5$ film with $S = 0.80$ formed on Cr(100) underlayer at 500 °C.

evaluated by comparing the intensity ratio of $SmNi_5(0001)$ to $SmNi_5(0002)$ reflection. The intensity (I) is proportional to structure (FF^*), Lorentz-polarization (L), and absorption (A) factors [18]. Here, I is a product of integrated intensity multiplied by the full with at half maximum of rocking curve measured for the reflection. In the present paper, an influence of temperature factor, which is often omitted when comparing two reflection intensities, is not considered. $F_{(0001)}$ and $F_{(0002)}$ are respectively $S(f_{Sm}-f_{Ni})$ and $f_{Sm}+5f_{Ni}$ [10], where f is the atomic scattering factor of Sm or Ni. Therefore, $I_{(0001)}/I_{(0002)}$ is expressed as

$$I_{(0001)}/I_{(0002)} = [\{S(f_{Sm}-f_{Ni})\}^2 LA]_{(0001)}/\{(f_{Sm}+5f_{Ni})^2 LA\}_{(0001)}. \quad (1)$$

By solving this equation, S is given as

$$S = (I_{(0001)}/I_{(0002)})\times[\{f_{Sm}+5f_{Ni}\}_{(0002)}/\{f_{Sm}-f_{Ni}\}_{(0001)}] \times[\{LA\}_{(0002)}/\{LA\}_{(0001)}\}]^{1/2}. \quad (2)$$

The S of films deposited at 400 and 500 °C are estimated to be 0.65 and 0.80, respectively. The S value improves with increasing the substrate temperature.

Figure 5 shows the magnetization curves measured for the film deposited at 500 °C. The film is easily magnetized when the magnetic field is applied along Cr[001] which is the direction between the c-axes of two $SmNi_5(11\bar{2}0)$ variants. On the other hand, the magnetization curve measured along Cr[011] saturates at a higher applied field of 10 kOe. The magnetization behavior is similar to the case of hcp-Co$(11\bar{2}0)$ film epitaxially grown on Cr(100) underlayer [19]. The in-plane anisotropy is thus considered to be reflecting the magnetic property of $SmNi_5$ crystal with the easy magnetization axis parallel to the c-axis.

4 Conclusion

$Sm_{17}Ni_{83}$ alloy films are deposited on Cr(100) underlayers by varying the substrate temperature in a range between 100 and 500 °C. The film growth behavior and the detailed film structure are investigated by RHEED and XRD. The films deposited above 400 °C consist of epitaxial $SmNi_5(11\bar{2}0)$ crystal, whereas the films deposited below the temperature consist of amorphous phase. As the substrate temperature increases from 400 to 500 °C, the order degree (S) increases from 0.65 to 0.80. Ordering of $SmNi_5$ phase is promoted with increasing the temperature. The ordered film shows an in-plane magnetic anisotropy reflecting the magnetic property of $SmNi_5$ crystal.

Acknowledgements

A part of this work was supported by JSPS KAKENHI Grant Number 25420294, JST A-STEP Grant Number AS242Z00169M, and Chuo University Grant for Special Research.

References

1. K. J. Strnat, *Handbook of Ferromagnetic Materials* (Elsevier Science B. V., New York, 1988)
2. A. Singh, R. Tamm, V. Neu, S. Fähler, W. Skrotzki, L. Schultz, B. Holzapfel, J. Appl. Phys. **97**, 093902 (2005)
3. E. E. Fullerton, J. S. Jiang, C. Rehm, C. H. Sowers, S. D. Bader, X. Z. Wu, Appl. Phys. Lett. **71**, 1579 (1997)
4. E. E. Fullerton, C. H. Sowers, J. P. Pearson, S. D. Bader, X. Z. Wu, D. Lederman, Appl. Phys. Lett. **69**, 2438 (1996)
5. M. J. Pechan, N. Teng, J. D. Stewart, J. Z. Hilt, E. E. Fullerton, J. S. Jiang, C. H. Sowers, S. D. Bader, J. Appl. Phys. **87**, 6686 (2000)
6. V. Neu, K. Häfner, L. Schultz, J. Magn. Magn. Mater. **322**, 1613 (2010)
7. M. Ohtake, T. Yanagawa, Y. Nonaka, F. Kirino, M. Futamoto, Proc. 22nd International Workshop on Rare-Earth Permanent Magnets and their Applications, Nagasaki, Japan, September 2012, pp. 166–169
8. M. Ohtake, Y. Nukaga, F. Kirino, M. Futamoto, J. Appl. Phys. **107**, 09A706 (2010)
9. A. K. Patra, V. Neu, S. Fähler, R. Groetzschel, S. Bedanta, W. Kleemann, L. Schultz, Phys. Rev. B **75**, 184417 (2007)
10. M. Seifert, L. Schultz, V. Neu, J. Appl. Phys. **106**, 073915 (2009)
11. O. Yabuhara, M. Ohtake, Y. Nukaga, F. Kirino, M. Futamoto, J. Phys.: Conf. Ser. **200**, 082026 (2010)
12. T. Yanagawa, M. Ohtake, F. Kirino, M. Futamoto, EPJ Web Conf. **40**, 06007 (2013)
13. M. Ohtake, O. Yabuhara, Y. Nukaga, F. Kirino, M. Futamoto, J. Appl. Phys. **107**, 09A708 (2010)
14. C. D. Paul W. E. Wallace, J. Appl. Phys. **39**, 5259 (1968)
15. A. Pasturel, C. Colinet, C. H. Allibert, P. Hicter, A. G. Percheron, J. C. Achard, Phys. Status Solidi B. **125**, 101 (1984)
16. K. H. J. Buschow, A. S. Van. Der. Goot, J. Less-Common. Met. **22**, 419 (1970)
17. G. Petzow, G. Effenberg, *Ternary alloys* (VCH Verlagsgesellschaft, Germany, 1993)
18. B. D. Cullity, *Elements of X-Ray Diffraction* (Addison-Wesley, Massachusetts, 1956)
19. A. Nakamura M. Futamoto, Jpn. J. Appl. Phys. **32**, L1410 (1993)